Nuclear Inst. and Methods in Physics Research, A 871 (2017) 148–153

Contents lists available at ScienceDirect

Nuclear Inst. and Methods in Physics Research, A

journal homepage: www.elsevier.com/locate/nima

Shape distortion of ^{128}I ß$^-$ spectrum observed by a self-activated CsI(Tl) scintillator for high-sensitivity neutron measurements

Soichiro Honda [a], Akihiro Nohtomi [b,*], Keita Machidori [c], Genichiro Wakabayashi [d]

[a] Diagnostic Imaging Center, Kurume University Hospital, 67 Asahi-machi, Kurume-shi, Fukuoka 830-001, Japan
[b] Graduate School of Medical Sciences, Kyushu University, 3-1-1 Maidashi, Higashi-ku, Fukuoka 812-8582, Japan
[c] Department of Health Sciences, Kyushu University, 3-1-1 Maidashi, Higashi-ku, Fukuoka 812-8582, Japan
[d] Atomic Energy Research Institute, Kindai University, 3-4-1 Kowakae, Higashiosaka-shi, Osaka 577-8502, Japan

ARTICLE INFO

Keywords:
Self-activation method
ß$^-$ spectrum of ^{128}I
ß$^-$-escape effect
γ-summing effect
Light collection efficiency
Optimum crystal size

ABSTRACT

The factors causing the distortion of the ^{128}I ß$^-$ spectrum detected by a self-activated CsI(Tl) scintillator were studied to verify the correctness of the spectral shape and the appropriateness of the discrimination setting for ß$^-$-particle counting by the scintillator. These criteria are essential for the correct evaluation of radioactivity generated in a scintillator volume by the self-activation method, which was recently proposed by our group.

A pulse height defect caused by the partial escape of ß$^-$ particles from the surface of the scintillator crystal shifts the ß$^-$ spectrum toward the lower-energy region when smaller CsI(Tl) scintillators are used (the ß$^-$-escape effect). For larger CsI(Tl) scintillators, an increase in pulse height caused by the summing of 0.443 MeV prompt γ-rays from the excited state of the ^{128}I daughter nuclide (^{128}Xe) affects the shape of the ß$^-$ spectrum considerably, resulting in a shift toward the higher-energy region (the γ-summing effect). The extent of the contributions of these two effects was examined by a Monte Carlo simulation of various cubical CsI(Tl) crystals of different sizes. It was found that the distortions caused by those two effects effectively cancel each other out for a medium-size cubical CsI(Tl) crystal with a side length of approximately 3 cm. This finding is very useful for the practical applications of the self-activation method.

In addition to the factors mentioned above, the efficiency of scintillation light collection by the photodetectors also affects the shape distortion of the ß$^-$ spectrum slightly through spectral line broadening due to the degradation of the energy resolution. This effect was estimated using a simple model with different discrimination settings for ß$^-$ pulse counting.

1. Introduction

A novel self-activation method using an iodine-containing scintillator was proposed in our previous papers [1–4] for highly sensitive detection of rather weak photoneutrons, primarily around a medical linear accelerator (linac). In the proposed method, in contrast with conventional activation detectors, the target material of the activation reaction is a major constituent of the detection medium, so that the activation product is contained in the detector as an internal source. Consequently, almost all of the ß$^-$ particles emitted from ^{128}I are stopped entirely in the scintillator and are counted efficiently by the scintillator. In this approach, the proper discrimination energy for ß$^-$ particle counting can be chosen by referring to the actual ß$^-$ spectrum detected by the same scintillator, for example, NaI(Tl) or CsI(Tl). The correct discrimination energy setting is essential for precise determination of the counting efficiency of ß$^-$ particles emitted from ^{128}I because some signals are not counted when the pulse height does not reach the discrimination level.

According to our previous measurements using medium-size scintillation crystals, approximately a few centimeters in diameter or height (for cylinders) or in side length (for cubes), the observed ^{128}I ß$^-$ spectra agree reasonably well with the theoretical spectrum of ^{128}I given in ICRP 107 [5], as shown in Fig. 1. A slight disagreement of ~2 MeV may be attributed to the slightly insufficient energy resolution of the detector system, rather than to the pile-up of pulses due to a high counting rate, as discussed in detail below. Another discrepancy in the CsI(Tl) spectrum at less than 0.4 MeV is due to noise in the photodiode. This good agreement is crucial for obtaining the proper discrimination setting in the self-activation method and results primarily from the high detection efficiency of ß$^-$ particles as an internal source (~100%) as

* Corresponding author.
E-mail address: nohtomi@hs.med.kyushu-u.ac.jp (A. Nohtomi).

http://dx.doi.org/10.1016/j.nima.2017.04.013
Received 17 January 2017; Received in revised form 6 April 2017; Accepted 7 April 2017
Available online 7 April 2017
0168-9002/

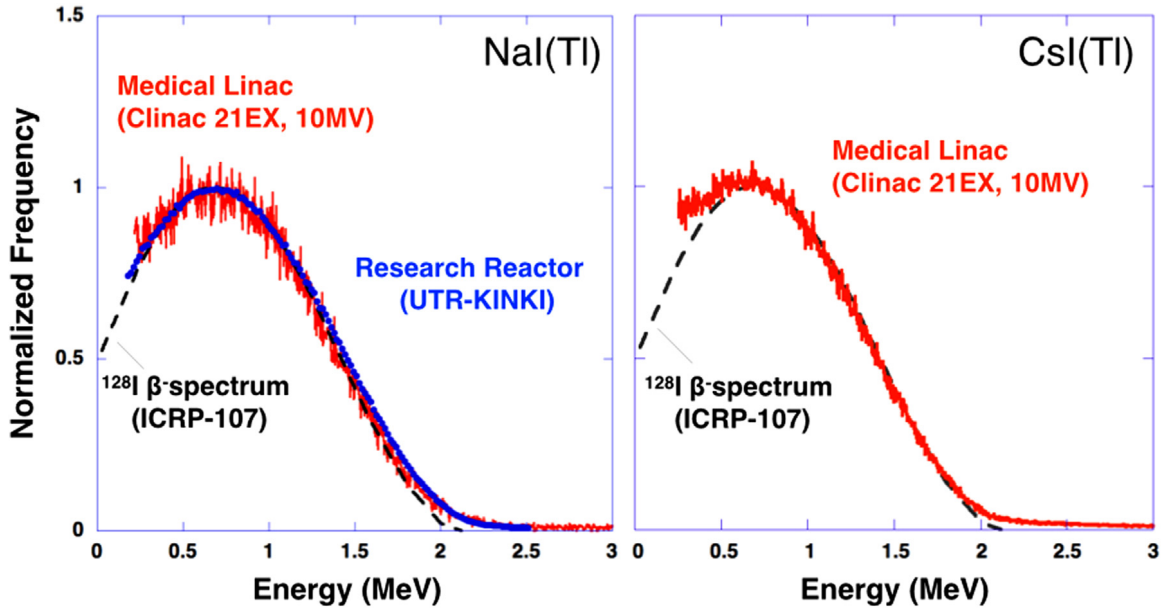

Fig. 1. Left: ß⁻ spectra of ^{128}I in a self-activated NaI(Tl) crystal (a cylinder with dimensions of ϕ 2.54 cm×2.54 cm) detected by the scintillator [1]. Right: Those in a self-activated CsI(Tl) crystal (a cube with a side length of 2.5 cm) [4]. Observed spectra are compared with the theoretical spectrum of ^{128}I given in ICRP 107 [5].

well as the reasonable uniformity of scintillation light collection in a relatively small crystal volume enclosed by high-reflectivity materials [6–8]. However, for much smaller or larger scintillators, non-negligible deviation from the theoretical spectrum would appear for several possible reasons.

In this paper, the factors responsible for shape distortion of the ^{128}I ß⁻ spectrum detected using a self-activated scintillator are studied using a Monte Carlo simulation. A simple model is used to verify the appropriateness of the discrimination setting for ß⁻-particle counting by the scintillator. A CsI(Tl) scintillator is selected as the main object of this study, as the use of CsI(Tl) instead of NaI(Tl) is expected to be advantageous in terms of manufacturing, handling, and costs. The optimum size of the CsI(Tl) crystal for the scintillator is determined according to the distortion of the ^{128}I ß⁻ spectrum detected by the scintillator.

2. Possible factors affecting shape distortion of ^{128}I ß⁻ spectrum observed by a self-activated CsI(Tl) scintillator

2.1. Escape of ß⁻ particles from scintillator surface: ß⁻ -escape effect

The range of electrons with the maximum ß⁻ energy of ^{128}I (2.12 MeV) is about 2.2 mm in a CsI(Tl) crystal. When ^{128}I is generated within 2.2 mm of the surface of CsI(Tl) as a result of self-activation by neutrons, some ß⁻ particles escape from the scintillator volume, and part of the initial energy is not deposited inside the CsI(Tl) crystal. This partial escape may distort the ß⁻ spectrum toward the lower-energy region, which we refer to as the ß⁻-escape effect. Consequently, a portion of the ß⁻-particle counts will be lost for a certain fixed discrimination energy. The distortion caused by the ß⁻-escape effect is more prominent for smaller scintillators because of their larger surface-area-to-volume ratio.

2.2. Summing of 0.443 MeV γ-rays from excited state of ^{128}Xe: γ-summing effect

After ß⁻ disintegration of ^{128}I, as shown in Fig. 2 [9], the daughter nuclide ^{128}Xe remains in its excited state (0.443 MeV) with a branching ratio of 11.6%, and a 0.443 MeV prompt γ-ray is emitted. Some portion of these 0.443 MeV γ-rays will be absorbed by the scintillator. Adding them to the pulse height of the ß⁻ signals may considerably affect the shape of the ß⁻ spectrum, resulting in a shift toward the higher-energy region, which we refer to as the γ-summing effect. For a fixed discrimination energy, this effect may increase the number of incorrect ß⁻ particle counts. The γ-summing effect is stronger for larger CsI(Tl)

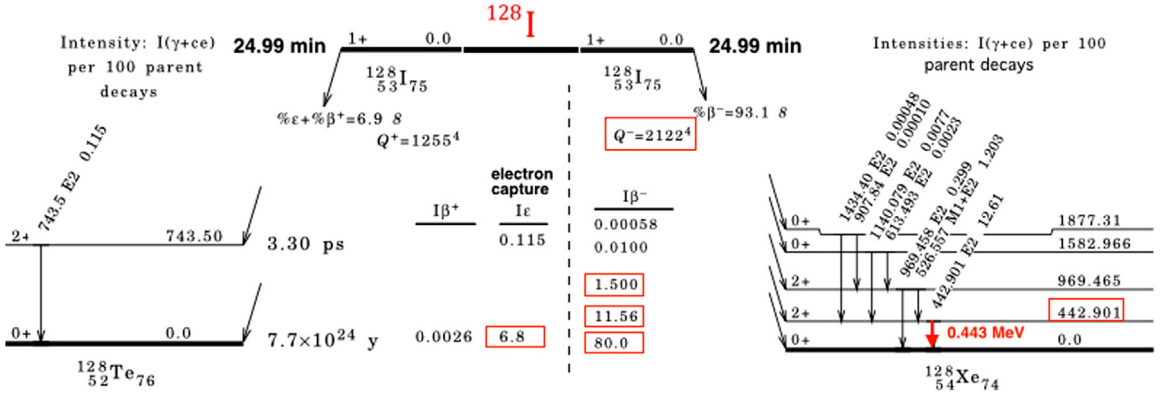

Fig. 2. Disintegration scheme of ^{128}I [9].

scintillators. Additionally, the γ-summing and ß⁻-escape effects shift the energy of the ß⁻ spectrum in opposite directions.

As illustrated in the disintegration scheme in Fig. 2, ^{128}Te is also generated as another daughter nuclide of ^{128}I through electron capture or ß$^+$ disintegration. The branching ratio is about 7%, and electron capture is dominant (the ß$^+$ disintegration is almost negligible). After the electron capture process, characteristic X-rays or Auger electrons are emitted. They are insignificant here because their energy is at most 27.5 keV, and the electron capture and ß$^+$ disintegration do not coincide with the ß⁻ disintegration.

2.3. Efficiency of scintillation light collection: energy-resolution effect

When ß⁻ particles are detected by a scintillator, low light-collection efficiency may broaden the continuous spectrum. As already mentioned, the slight disagreement between theory and experiment around 2 MeV in Fig. 1 is attributable to this effect, rather than to the pulse pile-up effect. This is because the slight disagreement remained even when the counting rate was considerably reduced from about 10 kcps (research reactor irradiation) to about a few hundred cps (medical linac irradiation).

The efficiency of scintillation light collection is determined primarily by the ratio of the photodetector area covering the scintillator surface (d) to the total scintillator surface area (S), as described by Hull et al. [6] (see Fig. 3). For example, in our previous experimental observations (Fig. 1), the bottom face of a ϕ2.54 cm × 2.54 cm NaI(Tl) crystal cylinder is coupled to a ϕ 5.08 cm photomultiplier (i.e., d is the area of a circle with a diameter of 2.54 cm) or the face of a CsI(Tl) crystal cube with a side length of 2.5 cm is coupled to a 2.8×2.8 cm^2 photodiode detector (d is the area of a square with a side length of 2.5 cm). In both cases, the ratio d/S is $1/6 \approx 0.167$, and, from Fig. 3, the light collection efficiency is about 90%. The efficiency of scintillation light collection directly affects the energy resolution of monoenergetic photon (γ-ray) detection, and the corresponding photopeak indicates broadening [6].

As a result of this spectral line broadening, when the fixed discrimination level is chosen to be smaller than the peak energy of the ^{128}I ß⁻ spectrum (~0.7 MeV), a portion of the ß⁻ pulses with energies larger than the discrimination level may effectively shift to the energy region below the discrimination level and not be counted. Conversely, if the fixed discrimination level is chosen to be larger than the peak energy of the spectrum, a portion of the ß⁻ pulses with energies smaller than the fixed discrimination level may shift to the higher-energy region and exceed the discrimination level. This impact of spectral line broadening on ß⁻-particle counting may be minimized and become almost negligible if a discrimination level around the peak energy is chosen.

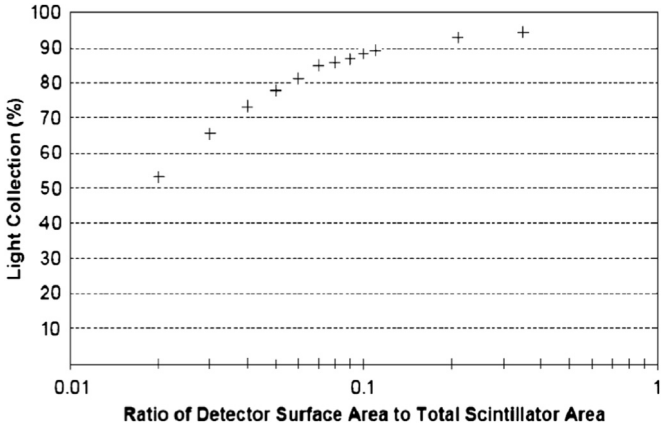

Fig. 3. Efficiency of scintillation light collection as a function of the ratio of the photodetector area covering the scintillator surface (d) to the total scintillator surface area (S) (Fig. 6 of Ref. [6]).

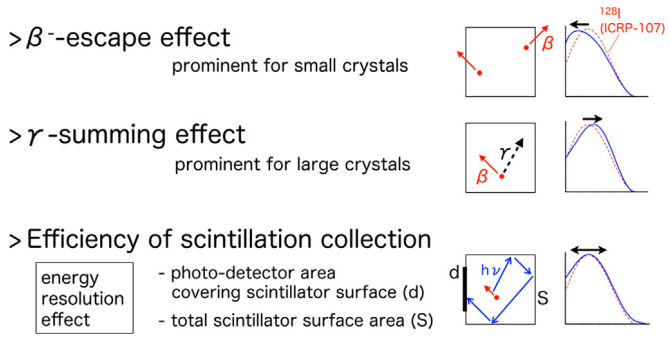

Fig. 4. Possible causes of distortion of ^{128}I ß⁻ spectrum.

All three of the factors that can potentially contribute to the distortion of the ^{128}I ß⁻ spectrum are schematically illustrated in Fig. 4.

3. Evaluation of the impact of spectral distortion on ß⁻ particle counting

3.1. Method of evaluating the impact of the ß⁻-escape effect

The energy deposited in a CsI(Tl) crystal by ß⁻ particles emitted from ^{128}I was calculated by a Monte Carlo code to evaluate the distortion of the energy spectrum by the ß⁻-escape effect for self-activated CsI(Tl) cubes with side lengths ranging from 1 to 5 cm. ^{128}I radiation sources were arranged uniformly inside a CsI(Tl) cube. The ß⁻ energy spectrum of ^{128}I was obtained using the theoretical spectrum of ^{128}I given in ICRP 107 as a reference [5]. PHITS version 2.81 [10] was used to calculate the energy deposited in the CsI(Tl) cube from its [T-deposit] tally.

3.2. Method of evaluating the impact of the γ-summing effect

In addition to the ß⁻-escape effect, the γ-summing effect was also taken into account. To calculate the combined effect, we divided the theoretical β^- spectrum of ^{128}I given in ICRP 107 [5] into two components with maximum energies of 1.68 MeV (branching ratio of 11.6% for ^{128}I) and 2.12 MeV (branching ratio of 80% for ^{128}I). Accordingly, the energy distribution of the ^{128}I ß⁻ particle was prepared using the e-type subsection in PHITS version 2.81 as two different ß⁻ spectra with maximum energies of 1.68 and 2.12 MeV. The ß⁻ spectrum with a maximum energy of E_{max}, $P(E; E_{max})$, was calculated on the basis of the Fermi theory using the Fermi function [11] as follows:

$$P(E;\ E_{max}) = pW(E_{max} - E)^2 \cdot F(Z,W) \cdot C(E), \quad (1)$$

where p is the momentum of the emitted electrons ($p = \sqrt{W^2 - 1}$), W is the total energy of an electron [$W = (E + m_0c^2)/m_0c^2$, where m_0c^2 is the electron's rest mass energy], $F(Z, W)$ is the Fermi function, and $C(E)$ is the correction factor for the spectrum [$C(E) = 1$ for an allowed transition].

We arranged ^{128}I radiation sources uniformly inside a CsI(Tl) cube. Then, the energy deposited in the CsI(Tl) scintillator was calculated separately for each of the two components with E_{max} = 1.68 and 2.12 MeV using the [T-Deposit] tally. Following the ß⁻ disintegration of E_{max} = 1.68 MeV, 0.443 MeV γ-rays were generated in the PHITS simulation, and the resultant energy depositions were summed with those made by ß⁻ particles when the 0.443 MeV γ-rays interacted with CsI(Tl). Finally, the separately calculated spectra of the two components were weighted by their branching ratios for ^{128}I and summed to obtain the actual ß⁻ spectrum of self-activated CsI(Tl) crystal cubes with side lengths ranging from 1 to 10 cm.

3.3. Method of evaluating the impact of the scintillation light collection efficiency

As already stated, the efficiency of scintillation light collection (i.e., the energy resolution of a scintillation detector) affects the ß⁻-particle counting by broadening the spectral line. The total number of photoelectrons generated in the incident layer of the photodetector (such as the photomultiplier and photodiode) coupled to a scintillator is given by

$$N = E\varepsilon\xi\delta, \tag{2}$$

where E [MeV] is the energy deposited in the scintillator by a ß⁻ particle, ε [photons/MeV] is the average number of scintillation photons emitted per unit energy deposition, ξ is the efficiency of light collection, and δ is the quantum efficiency of the incident layer of the photodetector. Assuming that the Poisson statistics is valid, the standard deviation σ of the number of photoelectrons is expressed as $\sqrt{N}$. For a given geometry of the scintillator and photodetector, expressed by d/S, ξ (d/S) is obtained from Fig. 3. Using this value of ξ , the response of a detector, P_G, to a monoenergetic deposition with energy E is obtained from a Gaussian distribution as follows:

$$\sigma = \sqrt{N} = \sqrt{\varepsilon\xi(d/S)\delta}\sqrt{E} = A\sqrt{E}, \tag{3}$$

$$P_G(x; E, d/S) = \frac{1}{\sigma\sqrt{2\pi}} \exp\left\{-\frac{1}{2}\left(\frac{x-E}{\sigma}\right)^2\right\}. \tag{4}$$

When E is expressed in MeV, the value of A $(=\sqrt{\varepsilon\xi(d/S)\delta})$ in Eq. (3) that reproduces the results obtained using a 2.5 cm cubical CsI(Tl) scintillator [d/S =0.167 and ξ (d/S) =0.93] for ^{137}Cs γ-rays is experimentally determined to be 0.045 $(\sqrt{\text{MeV}})$. The corresponding spectral line broadening was evaluated by convolving the response of a detector to a monoenergetic deposition [Eq. (4)] with the theoretical spectrum of ^{128}I given in ICRP 107 using Mathematica [12]. In the actual calculation, the ß⁻ spectrum of ^{128}I was divided into a series of fine energy bins with a width of 0.01 MeV, and each bin was approximated by the `UnitBox[]` function. Then, the broadening of each `UnitBox[]` function was estimated by applying the `Convolve[]` function with Eq. (4) to obtain the actual energy spectrum.

4. Results and discussion

4.1. Impact of the ß⁻-escape and γ-summing effects

The obtained results for the impact of the ß⁻-escape effect are shown in Fig. 5, which displays the calculated ^{128}I ß⁻ spectra normalized to their maximum values for cubical CsI(Tl) crystals of different sizes. Distortion of the ß⁻ spectrum toward the lower-energy region is prominent for small scintillators. The center-of-gravity energies for the ß⁻ spectra in Fig. 5 are plotted in Fig. 6 for cubical CsI(Tl) crystals of different sizes. Fig. 6 shows that the energies are smaller for smaller crystals.

When both the ß⁻-escape and γ-summing effects are simultaneously taken into account, as shown in Fig. 7, the distortion of the ß⁻ spectrum due to the ß⁻-escape effect (Fig. 5) is effectively moderated by the addition of the γ-summing effect. To confirm the validity of these calculations, the curve for L =1 cm in Fig. 7 is compared with an energy spectrum experimentally observed using a 1 cm cubical CsI(Tl) crystal that was irradiated in a nuclear reactor. As shown in Fig. 8, the observed and calculated curves show good agreement when the ß⁻-escape and γ-summing effects are taken into account.

The correction factor (CF) is calculated for ß⁻-particle counting by comparing the evaluated spectra in Fig. 7 and the theoretical β^- spectrum of ^{128}I (ICRP 107). For a fixed discrimination level, the CF is given by the ratio of the integrated ICRP spectrum to the integrated evaluated spectrum. The results are plotted in Fig. 9, which clearly shows that the distortions caused by these two effects tend to cancel each other out. In practical terms, this means it is not necessary to correct for these two effects for CsI(Tl) crystals with dimensions of about 2–5 cm if the discrimination level is less than 0.5 MeV.

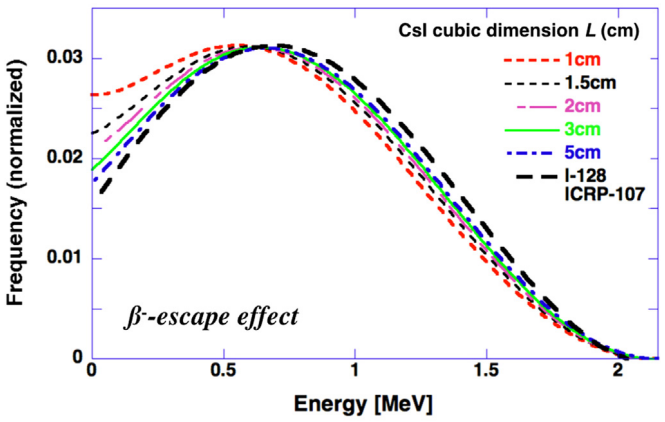

Fig. 5. Distortion of the ß⁻ spectrum toward the lower-energy region owing to the ß⁻-escape effect.

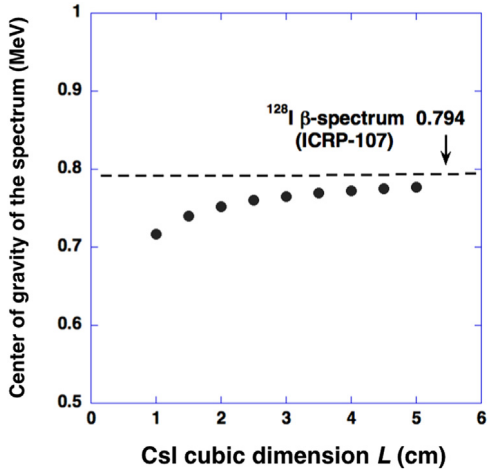

Fig. 6. Center-of-gravity energies of the ß⁻ spectra plotted in Fig. 5.

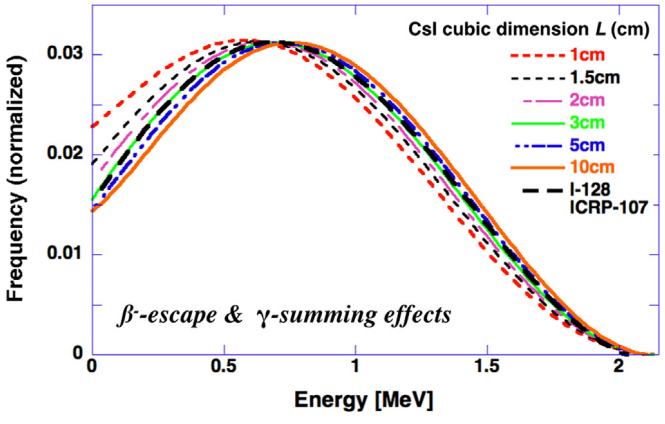

Fig. 7. Distortion of the ß⁻ spectrum due to both the ß⁻-escape and γ -summing effects.

4.2. Impact of the energy-resolution effect on the efficiency of scintillation light collection

The theoretical β^- spectrum of ^{128}I (ICRP 107) was convolved using a Gaussian distribution having $\sigma = A\sqrt{E(\text{MeV})}$ with A = 0.045 $(\sqrt{\text{MeV}})$ to evaluate the spectral line broadening caused by

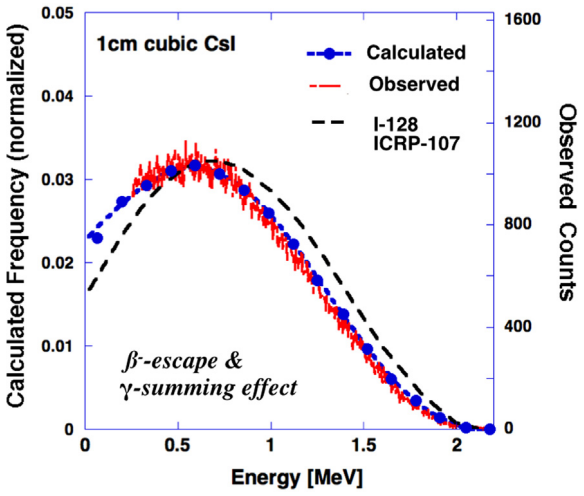

Fig. 8. Comparison of the calculated result for $L = 1$ cm in Fig. 7 and the energy spectrum experimentally obtained using a cubical CsI(Tl) crystal with a 1 cm side length after reactor irradiation.

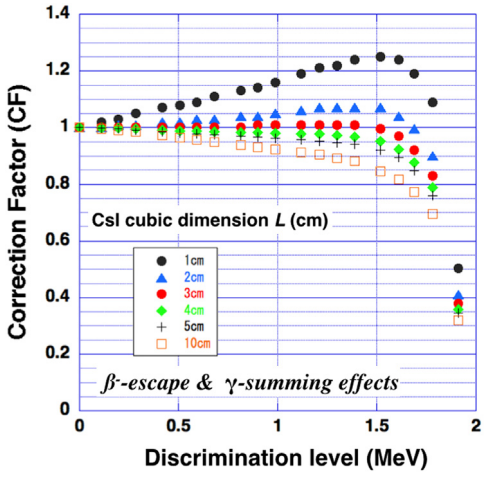

Fig. 9. Calculated correction factor (CF) of ß⁻-particle counting compensated for the impact of spectral distortion due to both the ß⁻-escape and γ -summing effects.

the energy-resolution effect for a 2.5 cm cubical CsI(Tl) crystal. The resultant energy spectrum is shown in Fig. 10. A slight disagreement with the theoretical distribution appears in the energy regions $E <$ 0.6 MeV and $E >$ 1.7 MeV as a result of the spectral line broadening, which is consistent with the experimental data presented in Fig. 1.

This deviation from the theoretical β^- spectrum of ^{128}I affects the ß⁻-particle counting for a fixed discrimination level, causing some incorrect counting. Therefore, appropriate corrections may be necessary. Consequently, another correction factor (CF′) was calculated by comparison with the theoretical β^- spectrum of ^{128}I. For a certain discrimination energy, CF′is given by the ratio of the integrated ICRP spectrum to the integrated convolved spectrum. As shown in Fig. 11, if a discrimination level of exactly 0.9 MeV is chosen, CF′equals 1, and no correction is necessary for this effect. Note that the magnitude of the correction does not exceed 1% as long as the discrimination level does not exceed 1.1 MeV.

5. Conclusion

Several significant factors causing shape distortion in the ^{128}I ß⁻ spectrum observed by a self-activated scintillator were studied. A Monte

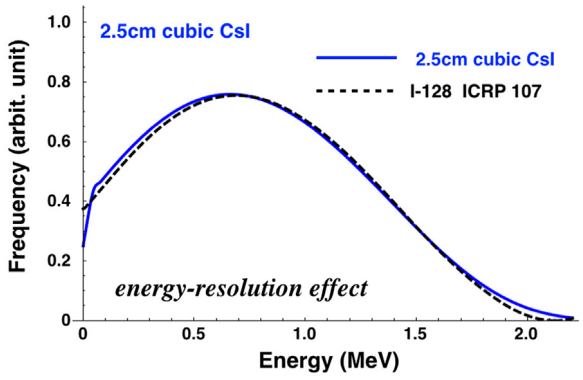

Fig. 10. Evaluated broadening of the theoretical β^- spectrum of ^{128}I (ICRP 107) due to the impact of the efficiency of scintillation light collection.

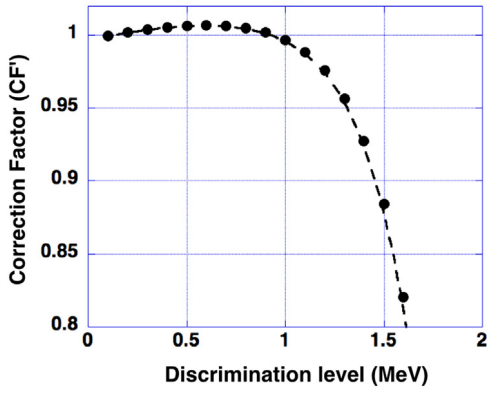

Fig. 11. Calculated correction factor (CF′) of ß⁻-particle counting compensated for the impact of spectral line broadening due to the energy-resolution effect.

Carlo simulation revealed that the shape distortions caused by the ß⁻-escape and γ-summing effects tend to effectively cancel each other out. By considering CsI(Tl) crystals of various sizes, the optimum side length of a CsI(Tl) cube at which the two effects were almost completely canceled was found to be around 3 cm. This means that it is not necessary to correct for these two effects for CsI(Tl) crystals with dimensions of approximately 2–5 cm. This fact is very helpful for the use of the self-activation method. In addition, a simple model was applied to verify the appropriateness of the discrimination setting for ß⁻-particle counting using a CsI(Tl) scintillator. The impact of the spectral line broadening caused by the energy-resolution effect on the ß⁻-particle counting was evaluated. It was determined that the correction does not exceed 1% if the discrimination level is set to 1.1 MeV or lower for a cubical CsI(Tl) scintillator with a side length L of 2.5 cm.

Conflict of interest

The authors declare that they have no conflict of interest.

Acknowledgment

The authors are grateful to Dr. K. Fushimi (Tokushima University) for his valuable comments on light collection in a scintillator. This work was partially supported by JSPS KAKENHI Grant Number JP16K10320.

References

[1] G. Wakabayashi, A. Nohtomi, et al., Radiol. Phys. Technol. 8 (2015) 125–134.
[2] A. Nohtomi, G. Wakabayashi, Nucl. Instrum Methods Phys. A 800 (2015) 6–11.

[3] A. Nohtomi, et al., Nucl. Instrum Methods Phys. A 832 (2016) 21–23.
[4] A. Nohtomi, et al., JPS Conf. Proc. 11 (2016) 050002.
[5] ICRP, Nuclear Decay Data for Dosimetric Calculations, ICRP Publication 107, Ann. ICRP (2008) p. 38.
[6] G. Hull, et al., Nucl. Instrum Methods Phys. A 588 (2008) 384–388.
[7] G.F. Knoll, Radiation Detection and Measurement, 4th ed, Wiley, New Jersey, 2010, 767.
[8] Comments by Dr. K. Fushimi, Tokushima University, private communication.
[9] Z. Elekens, J. Timar, Nuclear data sheets for A =128, Nucl. Data Sheets 129 (2015) 191–436.
[10] T. Sato, et al., J. Nucl. Sci. Technol. 50 (2013) 913–923.
[11] S. Fukano, Radioisotopes 51 (2002) 392–399.
[12] Wolfram Research, Mathematica 7, technical documentation; <http://reference.wolfram.com/> (2017.1.1).